Direct amplification of a nanosecond laser diode in a high-gain diode-pumped Nd:YVO4 amplifier

Xavier Délen, François Balembois, Patrick Georges

Direct amplification of a nanosecond laser diode in a high gain diode-pumped $Nd:YVO_4$ amplifier

Xavier Délen, François Balembois,* and Patrick Georges

Laboratoire Charles Fabry, UMR 8501, Institut d'Optique, CNRS, Université Paris-Sud, 2 Avenue Augustin Fresnel, 91127 Palaiseau Cedex, France

**Corresponding author: francois.balembois@institutoptique.fr*

Received November 4, 2013; revised December 17, 2013; accepted December 25, 2013; posted January 2, 2014 (Doc. ID 200658); published February 12, 2014

We demonstrate that $Nd:YVO_4$ can efficiently amplify a nanosecond laser diode in a very simple double-pass configuration. Based on longitudinal pumping with a high brightness fiber-coupled laser diode at 808 nm (60 W, 100 μm, 0.22 NA) and a low Nd-doped (0.2%) temperature controlled $Nd:YVO_4$ we achieved an optical gain of 62 dB with very low (<2%) parasitic laser emission and an average output power of 10 W. At 15 kHz, we observed a strong gain saturation dynamic resulting in a pulse duration reduction from 100 to 3.5 ns. This effect enhances the peak power by a factor of 18 (130 kW) with an energy of 620 μJ. © 2014 Optical Society of America

OCIS codes: (140.3280) Laser amplifiers; (140.4480) Optical amplifiers; (140.3480) Lasers, diode-pumped; (140.3530) Lasers, neodymium; (140.3538) Lasers, pulsed.

http://dx.doi.org/10.1364/OL.39.000997

A wide range of laser sources based on master oscillator power amplifier (MOPA) architectures require high gain amplifiers in order to amplify low power seed sources like pulse picked mode-locked oscillators, microchip lasers, or pulsed laser diodes. The latter are certainly the most versatile and compact seed sources since repetition rate and pulse duration can be adjusted on demand with the driving current. However, they also produce limited energy per pulse because of the very short carrier lifetime in semiconductors. Consequently, MOPAs with pulsed laser diodes generally require very high optical gain, typically in the 60 dB range. This can be achieved with multistage fiber amplifiers [1–3], which offer the possibility of building compact systems. However, nonlinear effects, such as stimulated Raman scattering, stimulated Brillouin scattering, or self phase modulation limit the output peak power of these systems in the pulsed regime [4]. Photonic crystal optical fibers with large mode areas have been developed in order to overcome these limitations by reducing the intensity [5]. Although they allowed significant improvement of the performance, output energies and peak power are still limited at a lower level than with diode-pumped bulk crystals. For example, regenerative amplifiers with diode pumped bulk crystals can be an alternative to multistage fiber amplifiers. They can provide high optical gain over 60 dB and can handle peak powers of several MW as well as multi-millijoule pulse energies [6,7]. However, the seed signal repetition rate is limited to a few hundred kHz and the pulse duration must be significantly shorter than the cavity round trip time. Moreover, these systems require the use of a high voltage power supply for the pockel cell that makes them relatively complex and expensive. A geometrical multipass bulk amplifier can also be considered as an alternative in order to obtain high gain amplification. The main challenge with this approach is to manage to obtain a large optical gain while keeping a simple setup.

Neodymium-doped yttrium orthovanadate ($Nd:YVO_4$) can be considered for this purpose with its remarkably high emission cross section of $12 \times 10^{-19}\ cm^2$ at 1064 nm [8]. Compared to Nd:YAG, the emission cross section time's lifetime product is over two times higher and can, therefore, produce a much higher optical gain. However, several studies have shown that the large emission cross section of $Nd:YVO_4$ is very sensitive to temperature changes [9–11]. It drops by over 50% for a temperature increase of 100 degrees, which has been found to be 2 to 3 times more than for Nd:YAG. It is, therefore, very important to minimize the temperature increase inside the crystal in order to design high gain amplifiers. The quantum defect and the associated heat load can be reduced by pumping at 880, 888, or even 914 nm rather than at 808 nm [12–14]. Several papers report significant power scaling of $Nd:YVO_4$ oscillators and efficiency improvement using this approach. For example, an output power of 60 W has been obtained with diode pumping at 888 nm [12]. However, for high inversion of population, as in the case of high gain amplifiers, our previous study shows that the thermal load can be minimized using 808 nm pumping [15]. Indeed, nonradiative transition rates increase strongly at the high doping concentrations needed to compensate for the lower absorption at 880, 888, or 914 nm.

$Nd:YVO_4$ amplifiers pumped at 808 nm have already been proven to deliver high gain. Output powers of around 10 W with gains of about 200 have been obtained with a two stage amplifier and a microchip laser or a fiber laser as seed source [16,17]. Using a more complex setup with a grazing incidence configuration with 4 pass and a phase conjugation mirror, a high gain of 41 dB has also been obtained with 26 W output power [18].

Choosing to work with a low doping concentration of 0.1 at. % and high brightness longitudinal 808 nm pumping configuration, we recently demonstrated similar results but with much simpler setup (single pass $Nd:YVO_4$ amplifier): an output power of 10 W with a pulse-picked $Nd:YVO_4$ picosecond seed source with an average power of 50 mW and a corresponding small signal gain of 45 dB [14].

Considering these past results, high gain amplification of pulses from a nanosecond laser diode with a very simple setup seems to be at hand. As amplifications of around 60 dB are needed, we designed a double pass-Nd:YVO_4 amplifier whose results are presented in this Letter.

As a seed source we use a single mode fiber-coupled DFB laser diode (ALPHANOV PDM). Its emission optical spectrum (below 0.1 nm at FWHM for 20 ns pulses) is narrower than the emission line of our crystal (0.8 nm), which allows it to fully benefit from the high emission cross section of Nd:YVO_4. Temperature tuning is done to set the emission wavelength at 1064.2 nm, which matches the gain maximum around room temperature. This laser diode can be operated in pulsed regime and delivers up to 275 mW of peak power and 36 mW of average power. It can produce nanosecond optical pulses with repetition rates up to 1 MHz, by direct current modulation. It also includes a fiber optical isolator with over 50 dB isolation. The optical setup of the amplifier is shown in Fig. 1. The output beam of the seeding laser diode is collimated and sent into two consecutive optical isolators. Although it was not completely necessary, the first bulk isolator was used to prevent any optical feedback in the seed source while exploring a wide range of settings. The second isolator allows for extraction of the signal after two passes through the crystal with the same polarization. A single lens is then used to focus the signal beam on a 350 μm diameter in the gain medium. The signal polarization is linear and aligned with the c axis of the crystal in order to benefit from the highest emission cross section. The laser crystal is an a-cut 20 mm long Nd:YVO_4 crystal with a doping concentration of 0.2 at. % and a 3 mm × 3 mm square section. The choice of the low doping concentration allows the spreading of the heat load over a longer length and reducing the probability of nonradiative decays [15]. This way, the local temperature increase can be reduced and we can benefit from a higher emission cross section. The crystal is held by two water cooled copper mounts in order to extract the heat. Both crystal facets are AR coated with a reflectivity below 0.1% at 1064 nm and below 0.5% at 808 nm. A 3° wedge on one of the facets prevents parasitic laser oscillation in the high gain operation regime of our amplifier. The pump beam is delivered by a fiber-coupled 60 W laser diode emitting at around 808 nm. Its output optical fiber has a core diameter of 100 μm and a numerical aperture of 0.22. Two doublets of 40 and 150 mm focal length allow for focusing the pump beam over a diameter of 375 μm inside the crystal. In order to combine the signal and pump beam, we use a dichroic mirror with high reflectivity at 1064 nm and high transmission at 808 nm at an angle of incidence of 45°. Finally, the signal beam waist is imaged on a HR-coated plane mirror using a 100 mm focal length lens in a 2f–2f configuration. Coming back through the incoming path, the amplified beam exits the system through the output port of the first optical isolator.

First, we study the behavior of our system with 10 ns pulses at a 1 MHz repetition rate. Fig. 2 shows how the double-pass optical gain (in dB) and the output power evolve as a function of the seed average power at the full pump power. In order to keep all the other seed laser beam parameters constant, the input power is modulated using a half-wave plate and a polarizer. The output power ranges from 8 to 15 W for seed powers between 1 μW and 2 mW. It corresponds to a remarkably high optical gain, between 39 and 69 dB. The maximum output power of 16.4 W is measured for an input power of only 2 mW. It corresponds to a gain of 39 dB and an optical efficiency of 27% with regard to the total pump power of 60 W. An output power of 10 W is reached for a seed power of only 10 μW, whereas a seed power of 50 mW was needed in the one pass configuration of our previous experiment [15]. The gain reaches a maximum of 68 dB for an input power of 1 μW. The pulse duration is between 8 and 9 ns after amplification. Fig. 2 also shows the beam profiles after amplification in far field and near field. The M^2 of the output beam is below 1.5 in both directions.

At these very high gain levels, the presence of parasitic laser oscillation and amplified spontaneous emission is likely and should be monitored. In the following, we will call "parasitic emission" the power measured at the output other than the amplified signal. In the pulsed regime, the power of the parasitic emission can be evaluated using a photodiode at the amplifier output. For a very low seed average power of 1 μW and a corresponding gain of 68 dB, we measured that parasitic emission represents 8% of the total output power. This value drops below 2% for seed powers above 5 μW, which corresponds to optical gains below 62 dB. These measurements show that our system can handle optical gains of over 60 dB without being limited by parasitic oscillation or amplified spontaneous emission. This is close to the gain that could be obtained using a regenerative amplifier, or at least 2

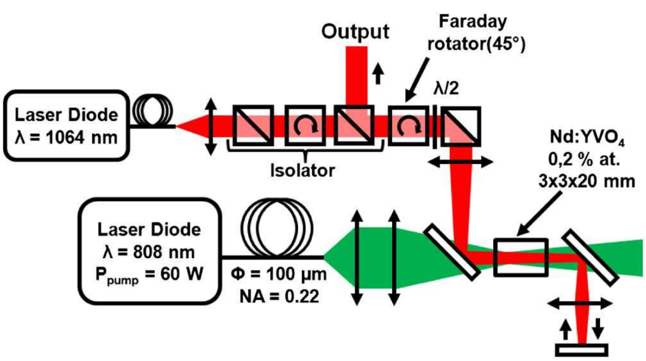

Fig. 1. Experimental setup.

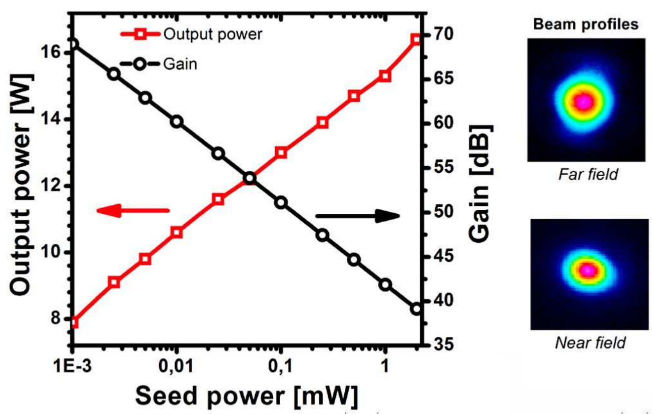

Fig. 2. Left: optical gain (dB) and output power (W) versus the seed power (mW) at full pump power (60 W in total) after a double pass in the Nd:YVO_4 crystal. Right: beam profiles in the near field and far field after amplification.

consecutive fiber amplification stages, indicating the high performances of our simple and optimized double-pass scheme.

Due to the differences in gain variations, we expect differences in parasitic emission power with the repetition rate. We compare different observations at high and low repetition rates. In the following, we will refer to the small signal gain at an instant in time as the "instantaneous gain" and to the ratio between average input and output power as the "average gain." At high repetition rates, the energy extracted by the amplification of the laser pulse is small compared to the stored energy. Consequently, instantaneous gain variations over a cycle between two pulses are also minimized in this regime. However, at lower repetition rates, the evolution of stored energy in the laser crystal induced by the pulse amplification can result in large gain variations over a cycle. Parasitic oscillation might, therefore, limit the performance of our amplifier at much lower average optical gains in these regimes. For example, Fig. 3 shows the output signal obtained for a seed power of 350 μW with 100 ns pulses at a repetition rate of 15 kHz. Parasitic emission appearing before the amplified pulse is clearly visible on the photodiode signal. It shows what seems to be relaxation oscillations, which clearly indicate the presence of an optical cavity and not only amplified spontaneous emission. In this case, parasitic emission represents 12% of the total output power at 15 kHz for an average gain of 44 dB. The ratio between the amplified pulse shape and the seeded one indicates that the instantaneous gain reaches a maximum of 70 dB just before the seed pulses arrive. The amplification of a seed pulse induces a decrease of the instantaneous gain by 27 dB. In contrast, we can estimate that the instantaneous gain fluctuations are only around 0.5 dB for a repetition rate of 1 MHz. It explains why the average gain can be much higher at 1 MHz (68 dB) than at 15 kHz (44 dB) without inducing more parasitic emission. In any case, the parasitic emission power ratio seems to become significant for peak gain values above 65 dB.

As can be seen in Fig. 4, the gain saturation dynamic also affects the temporal profile of the amplified pulses. At a repetition rate of 15 kHz, it results in a pulse duration shortening from 100 ns at FWHM down to only 3.5 ns. This induces a strong enhancement of the optical peak power, which reaches a maximum of over 130 kW for an output energy of 620 μJ. Assuming the seeded pulse temporal profile was conserved, the peak power would only reach 7 kW at this energy level.

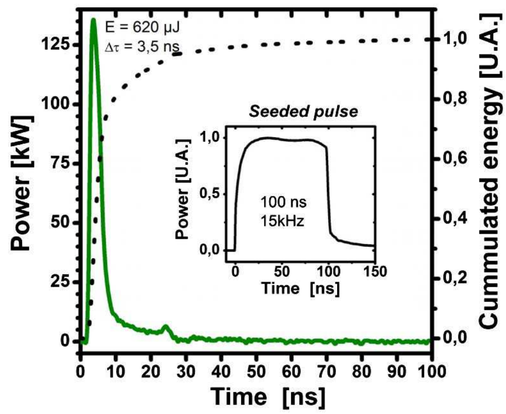

Fig. 4. Output pulse temporal profile for 100 ns duration seed pulses at a repetition rate of 15 kHz.

Figure 5 shows the evolution of the output power of the amplified pulses and the output pulse duration versus the repetition rate between 15 and 100 kHz. The seed signal has a constant average power of 350 μW and the seed pulses have a 100 ns FWHM duration. After amplification, the output pulse durations range from 3.5 to 13 ns. The pulse duration decrease can be fully explained by gain saturation dynamic at low repetition rate. However, at intermediate repetition rates such as 100 kHz, the pulse duration shortening is also due to the spectral chirp of the seeded pulses. A linear chirp of around 5 pm/ns is observed for 100 ns pulses with a peak current of 1.0 A.The output power varies between 9.2 and 13.3 W between 15 and 100 kHz because of the low excited state lifetime of $Nd:YVO_4$, which is only around 100 μs. This 33% decrease in output power is close to the −16% to −36% that has been observed at the output of a Q-switched oscillator for repetition rates between 20 and 100 kHz [19].

In conclusion, we have demonstrated a simple design of a double-pass $Nd:YVO_4$ passive amplifier with unprecedented performance. We obtained optical gains of 62 dB for 10 W output power with a single amplification stage without being limited by amplified spontaneous

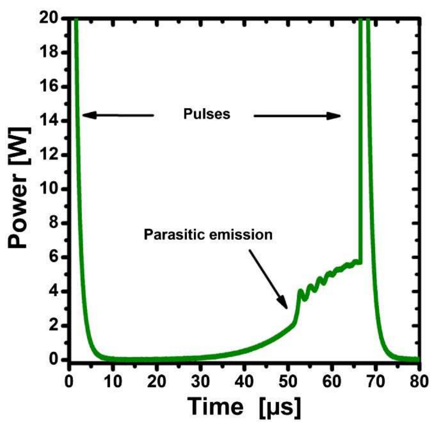

Fig. 3. Output power of the amplified beam versus time for 100 ns duration seed pulses at a repetition rate of 15 kHz.

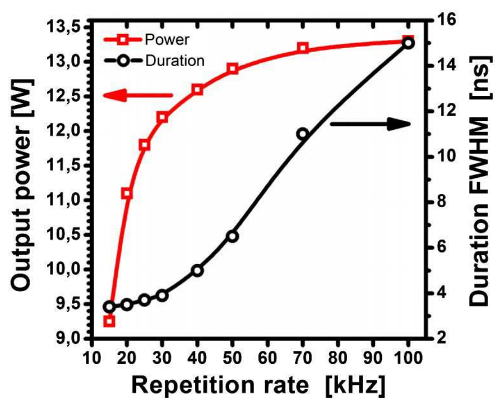

Fig. 5. Output power and output pulse duration at FWHM versus the repetition rate, for a constant seed average power of 350 μW.

emission. At low repetition rates we also showed that gain saturation dynamic can induce a strong enhancement of the peak power. This type of amplifier can potentially find many applications offering very high optical gain with a simple setup. Moreover, as it is based on bulk technology, it also has the capability to support higher pulse energies and higher peak power than conventional fiber amplifier systems.

The authors acknowledge the DGA , OSEO and Conseil Régional d'Ile de France for the funding of this research.

References

1. P. Dupriez, A. Piper, A. Malinowski, J. K. Sahu, M. Ibsen, B. C. Thomsen, Y. Jeong, L. M. B. Hickey, M. N. Zervas, J. Nilsson, and D. J. Richardson, IEEE Photon. Technol. Lett. **18**, 1013 (2006).
2. Y. Jeong, J. Nilsson, J. K. Sahu, D. N. Payne, R. Horley, L. M. B. Hickey, and P. W. Turner, IEEE J. Sel. Topics Quantum Electron. **13**, 546 (2007).
3. H. Liu, C. Gao, W. Zhao, and Y. Wang, Opt. Express **16**, 7888 (2008).
4. D. J. Richardson, J. Nilsson, and W. A. Clarkson, J. Opt. Soc. Am. B **27**, B63 (2010).
5. M. Laurila, M. M. Jørgensen, K. R. Hansen, T. T. Alkeskjold, J. Broeng, and J. Lægsgaard, Opt. Express **20**, 5742 (2012).
6. T. Metzger, A. Schwarz, C. Y. Teisset, D. Sutter, A. Killi, R. Kienberger, and F. Krausz, Opt. Lett. **34**, 2123 (2009).
7. M. Delaigue, I. Manek-Hönninger, F. Salin, C. Hönninger, P. Rigail, A. Courjaud, and E. Mottay, Appl. Phys. B **84**, 375 (2006).
8. A. W. Tucker, M. Birnbaum, C. L. Fincher, and J. W. Erler, J. Appl. Phys. **48**, 4907 (1977).
9. G. Turri, H. P. Jenssen, F. Cornacchia, M. Tonelli, and M. Bass, J. Opt. Soc. Am. B **26**, 2084 (2009).
10. X. Délen, F. Balembois, and P. Georges, J. Opt. Soc. Am. B **28**, 972 (2011).
11. Y. Sato and T. Taira, Opt. Mater. Express **2**, 1076 (2012).
12. L. McDonagh, R. Wallenstein, R. Knappe, and A. Nebel, Opt. Lett. **31**, 3297 (2006).
13. P. Zhu, D. Li, P. Hu, A. Schell, P. Shi, C. R. Haas, N. Wu, and K. Du, Opt. Lett. **33**, 1930 (2008).
14. D. Sangla, M. Castaing, F. Balembois, and P. Georges, Opt. Lett. **34**, 2159 (2009).
15. X. Délen, F. Balembois, and P. Georges, J. Opt. Soc. Am. B **29**, 2339 (2012).
16. A. Agnesi, L. Carrà, F. Pirzio, and G. Reali, Appl. Phys. B **109**, 659 (2012).
17. A. Agnesi, L. Carrà, R. Piccoli, F. Pirzio, and G. Reali, Opt. Lett. **37**, 3612 (2012).
18. K. Nawata, M. Okida, K. Furuki, K. Miyamoto, and T. Omatsu, Opt. Express **17**, 20816 (2009).
19. L. Mcdonagh and R. Wallenstein, Opt. Lett. **31**, 3303 (2006).